Emission temperatures and freeze out densities from light particle correlation functions in Au+Au collisions at 1 A·GeV

S.Fritz for the ALADiN collaboration:

R. Bassini,(2) M. Begemann-Blaich,(1) A.S. Botvina,(3)[1] S.J. Gaff,(4) C. Groß,(1) G. Immé,(5) I. Iori,(2) U. Kleinevoß,(1) G.J. Kunde,(4) W.D. Kunze,(1) U. Lynen,(1) V. Maddalena,(5) M. Mahi,(1) T. Möhlenkamp,(6) A. Moroni,(2) W.F.J. Müller,(1) C. Nociforo,(5) B. Ocker,(7) T. Odeh,(1) F. Petruzzelli,(2) J. Pochodzalla,(1)[2] G. Raciti,(5) G. Riccobene,(5) F.P. Romano,(5) Th. Rubehn,(1)[3] A. Saija,(5) M. Schnittker,(1) A. Schüttauf,(7) C. Schwarz,(1) W. Seidel,(6) V. Serfling,(1) C. Sfienti,(5) W. Trautmann,(1) A. Trzcinski,(8) G. Verde,(5) A. Wörner,(1) Hongfei Xi,(1)[4] and B. Zwieglinski(8)

(1)Gesellschaft für Schwerionenforschung, D-64291 Darmstadt, Germany
(2)Istituto di Scienze Fisiche dell' Università and I.N.F.N., I-20133 Milano, Italy
(3)Institute for Nuclear Research, Russian Academy of Sciences, 117312 Moscow , Russia
(4)Department of Physics and Astronomy and National Superconducting Cyclotron Laboratory, Michigan State University, East Lansing, MI 48824, USA
(5)Dipartimento di Fisica dell' Università and I.N.F.N., I-95129 Catania, Italy
(6)Forschungszentrum Rossendorf, D-01314 Dresden, Germany
(7)Institut für Kernphysik, Universität Frankfurt, D-60486 Frankfurt, Germany
(8)Soltan Institute for Nuclear Studies, 00-681 Warsaw, Hoza 69, Poland

Abstract

A study of emission temperatures extracted from excited state populations and of freeze out radii from light particle intensity interferometry is presented. Three high resolution ΔE–E–Hodoscopes with a total of 216 detectors are combined with the ALADiN setup in order to study Au+Au collisions at 1 A·GeV. In contrast to measurements with the isotope thermometer the extracted apparent temperatures do not vary with impact parameter thus with excitation energy. From the extracted radii a freeze out density was determined which decreases from $0.2\rho_0$ for the most peripheral to less than $0.1\rho_0$ for the most central collisions. A density–dependent feeding correction is applied to the different temperature measurements.

[1]Present Address: Bereich Theoretische Physik, Hahn-Meitner-Institut, D-14109 Berlin, Germany
[2]Present address: Max-Planck-Institut für Kernphysik, D-69117 Heidelberg, Germany
[3]Present address: Nuclear Science Division, Lawrence Berkeley Laboratory, Berkeley, CA 94720, USA
[4]Present address: NSCL, Michigan State University, East Lansing, MI 48824, USA

1 Introduction

In a recent publication [1] we presented the determination of emission temperatures and excitation energies in Au+Au collisions in order to explore the liquid-gas phase transition of nuclear matter. One open question was the influence of feeding on the isotope thermometer T_{HeLi}. In a follow up experiment we compared the isotope thermometer with temperatures derived from the relative yields of excited particle–unbound states. The idea was to calibrate the isotope thermometer with a temperature determined from the excited states rather than deriving this calibration from theoretical calculations.

The following excited state thermometers were analyzed:

1. ^{5}Li which decays into d–^{3}He ($E^* = 16.66$ MeV) and into p–α in the ground state.
2. ^{6}Li where the apparent temperature was determined by the ratio of the third ($E^* = 4.31$ MeV) and fifth ($E^* = 5.65$ MeV) excited states to the first ($E^* = 2.168$ MeV) excited state which all decay into d–α.
3. ^{8}Be where the ratio of the state at $E^* = 17.64$ MeV (decays into p–^{7}Li) to the state at $E^* = 3.04$ MeV (decays into α–α) is used for the temperature determination.

The paper is organized as follows:

In section 2 details of the experimental setup are given. The extracted temperatures for various event selection criteria are presented in section 3. Extracted radii and freeze out densities from p–p and d–α correlations are presented in section 4. In section 5 the results are compared to feeding calculations.

2 Experimental setup and data analysis

The experiment was performed at the SIS accelerator at GSI, Darmstadt. The experimental setup ist shown in Fig. 1. A 25 mg/cm^2 Au target was irradiated by a 1 A·GeV Au beam at a beam intensity of 10^6 particles per second. The forward hodoscope ZDO consisted of 36 phoswich detectors with a coverage of $6.5 < \theta < 21.5^0$ and $0 < \phi < 360^0$. Three small–angle high–resolution $\Delta E - E$–hodoscopes with a total of 216 elements were placed at laboratory angles $\theta = 100 - 150^0$. Each of the 216 elements consisted of a silicon detector of 300 μm thickness and a cesium iodide detector of 6 cm length for 160 detectors and 10 cm length for 56 detectors, read out by photodiodes. Isotopes were resolved for $Z = 1 - 4$. The energy calibration was performed according to [2] and an energy resolution of about 1% was achieved. From the cross calibration between detectors we got an additional smearing of 1% resulting in an overall uncertainty of $\approx 2\%$. The superposition of the ΔE–E distributions of all detectors is shown in Fig. 2. The separation of the Hydrogen isotopes (at $Z = 1$), the Helium isotopes (at $Z = 2$) and the Lithium isotopes (at $Z = 3$) is clearly visible.

The trigger required two valid hits in the ZDO and two valid hits in the combination of the three hodoscopes. For event characterisation we used the ALADiN Time-of-flight wall, which is described in detail elsewhere [3]. The variable Z_{bound} in the TOF array which is the summed charge in forward angles excluding the $Z = 1$ particles serves well as a

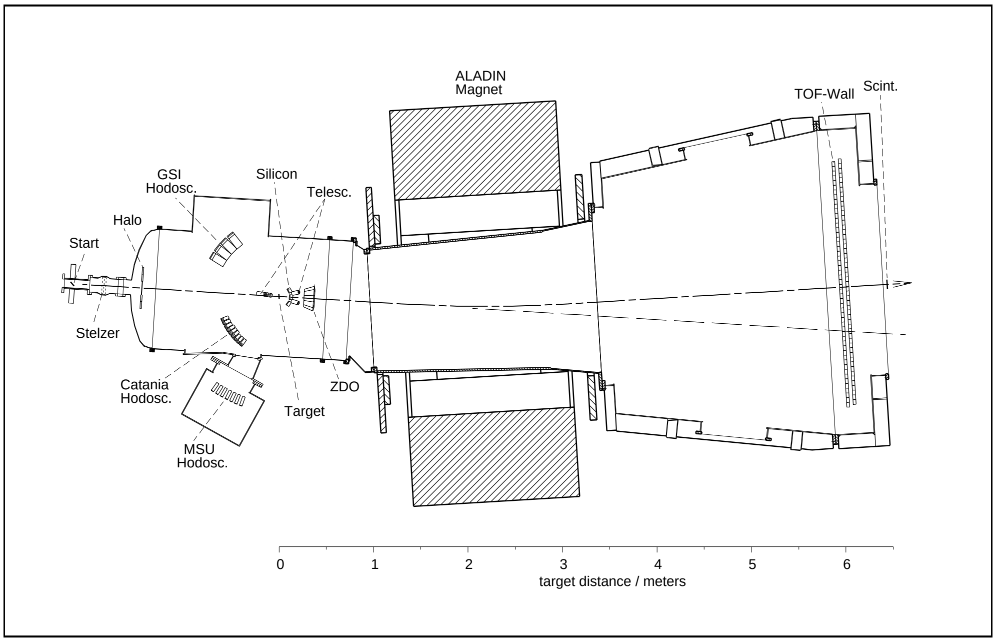

Figure 1: *Experimental setup*

criteria of the centrality of a collision [3]. Analogous event selection criteria as in [1, 3] were used. By the measurement of the decaying projectile spectator fragment charges with $Z \geq 2$i and the neutrons ([3]) an excitation energy E^* and a mass of the prefragment A_0 could be assigned to every Z_{bound} bin [4]. The mass of the prefragment A_0 was used in

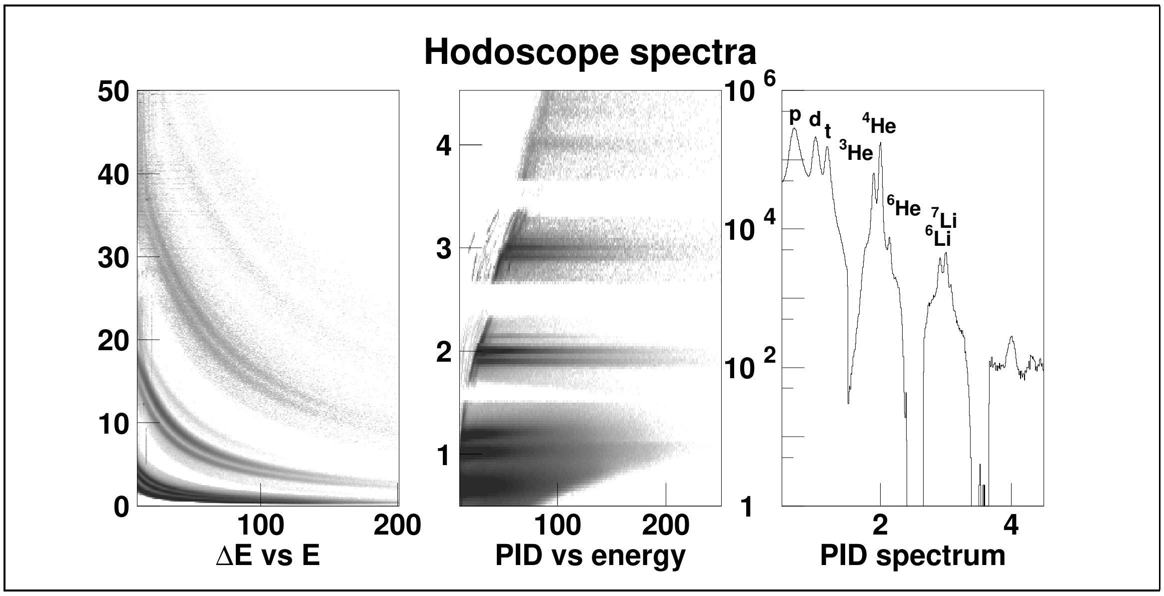

Figure 2: *ΔE vs E (left), PID vs energy in MeV (middle) and PID spectrum (right)*

the present analysis to extract the freeze out density from the radii derived by p–p and d–α correlations.
In Fig. 3 energy spectra for light particles together with moving source fits assuming three

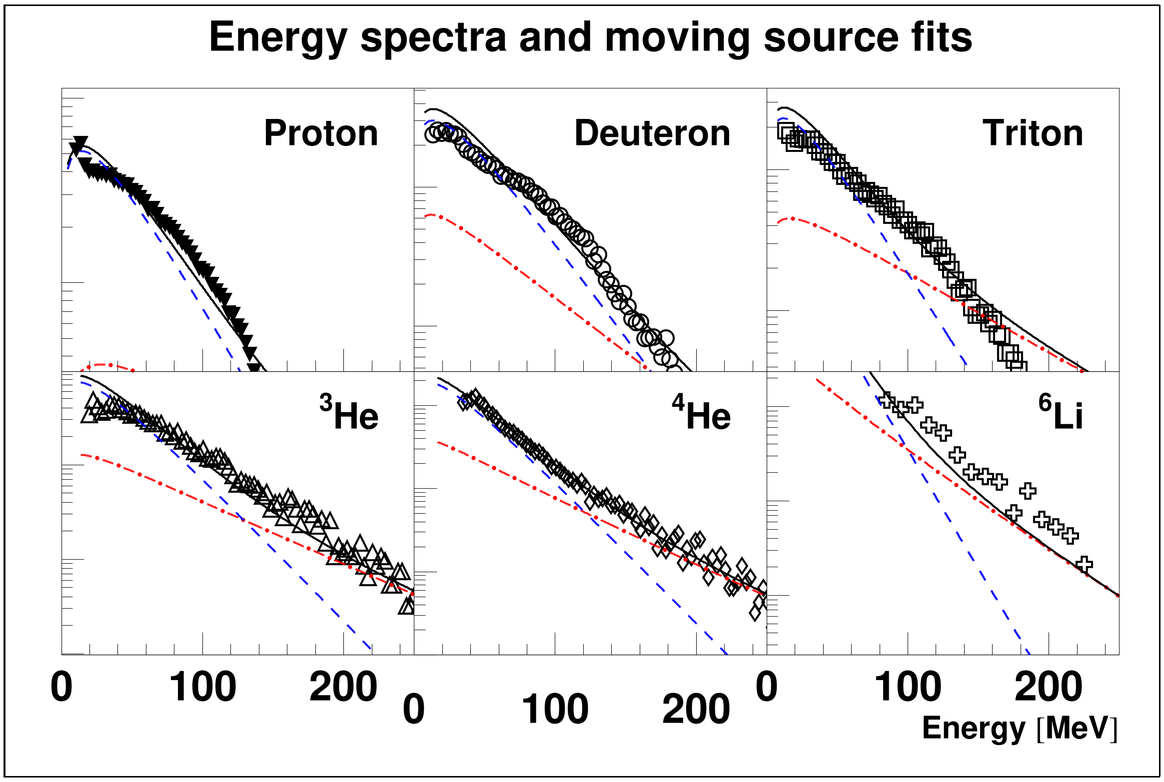

Figure 3: *Energy spectra at $\langle\theta\rangle = 35^0$ and 2 source fit for 1 A·GeV dashed lines ≡ target source, dot dashed lines ≡ midrapidity source*

sources in a symmetric system are presented. The moving source fits gives the following results:

1. The main contribution of the spectra can be described by a single source, the target source moving with less than 3% c in the laboratory frame.

2. The inverse slopes of the spectra decrease with increasing mass of the particle species even for the most central collisions.

3. The inverse slopes increase continuously with increasing centrality. This rise is partly due to the increase of bounce with decreasing impact parameter [4], partly to the increasing excitation energy with decreasing impact parameter. Its difference to temperatures extracted from isotope yields or excited states can be partly assigned to the effect of the Fermi motion [5] and to a significant part of pre–breakup emission of light particles [6].

In order to construct the correlation function for a specific particle pair one combines all particles of one species with all particles of the other species within one event and

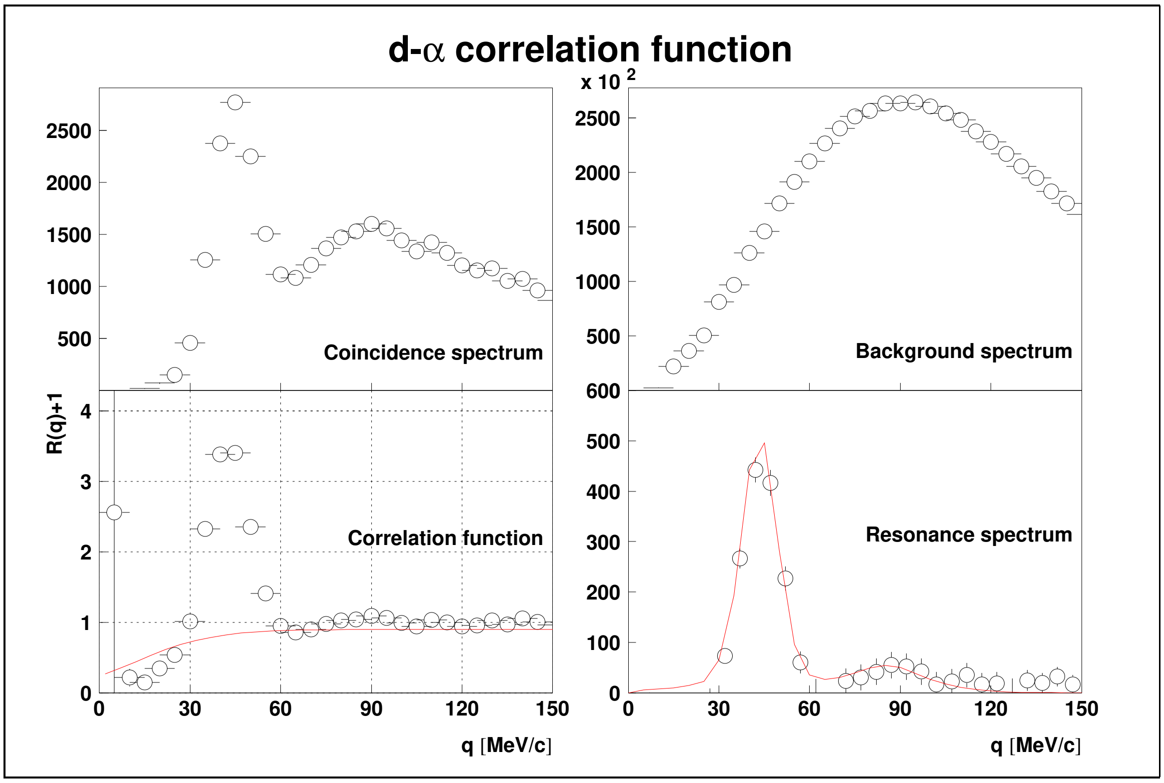

Figure 4: *Coincidence yield in the d–α correlation function (upper left), uncoincident yield from the event mixing technique (upper right), ratio of coincident and uncoincident yield (symbols) and assumed nonresonant part (line, lower left), extracted yield (symbols) compared with simulated yield (line, lower right)*

sorts the pairs according to their relative momenta. The coincidence spectrum shows the resonances of interest on top of a broad background distribution which is determined by phase space and acceptance of the hodoscopes. This background was determined with the event mixing technique [7], combining particles from different events. The correlation function is constructed by dividing the coincidence yield by the background yield and normalizing it to 1 for large relative momenta as shown in Fig. 4 for the d–α correlation function. For the determination of a temperature one is interested in the absolute yields of the different states. First, the nonresonant part of the correlation function has to be subtracted. This part comes from Coulomb repulsion and quantum mechanical effects and was determined by scaling non-resonant correlation functions like t–t or t–^{3}He. After subtracting this non resonant part of the correlation function and multiplying the resulting spectrum with the integral coincidence yield a resonance spectrum is derived. This is shown in the lower right panel of Fig. 4. The spectrum is compared to a Monte Carlo calculation for a certain emission temperature (here 5 MeV), which includes the first five excited states of ^{6}Li, the detection efficiency and resolution of the detector. Details of the Monte Carlo calculation are presented in Ref. [8].

3 Temperature extraction from excited states

Details of the level schemes for the analyzed thermometers are presented in table 1 For

Thermometer	Decay channel	SpinJ^{π}	Energy [MeV]	Γ[kev]	q[MeV/c]
^{5}Li	$p-\alpha$	$3/2^-$	G.S.	1500	54.3
	$d-^3$ He	$3/2^+$	16.66	200	24.7
^{6}Li	$d-\alpha$	3^+	2.17	24	41.5
	$d-\alpha$	2^+	4.31	1700	84.1
	$d-\alpha$	1^+	5.65	1500	99.1
^{8}Be	$\alpha-\alpha$	0^+	G.S.	6.8 eV	18.3
	$\alpha-\alpha$	2^+	3.04	1500	108
	$p-^7$ Li	1^+	17.64	10.7	27

Table 1: Level schemes of analyzed particle–unstable states (from [9])

the ^{5}Li thermometer the ratio of the first excited state at E^* =16.66 MeV to the ground state was used. The wide ground state was fitted with the R–matrix formalism with values taken from [9]. The two correlation functions together with a minimum and a maximum background are shown in the first row of Fig. 5. The well known peak of $^9\mathrm{B} \rightarrow p + {}^8\mathrm{Be}_{g.s} \rightarrow p + (\alpha + \alpha)$ just above threshold could not be resolved in the experimental correlation function. The apparent temperature for ^{5}Li and the other excited state thermometers is determined by fitting the yield ratios of simulated resonance spectra for a range of input temperatures to the experimental yield ratios and using to the exponential temperature formula

$$\frac{Y_2}{Y_1} = \frac{2J_2+1}{2J_1+1} \cdot \exp\left(-\frac{\Delta E}{T}\right) \tag{1}$$

^{8}Be decays in the ground and the first excited state into α–α, the fourth to sixth excited states decay into p+^{7}Li (Fig. 5 second row). The ground state (q = 18 MeV/c) is too close to the detection threshhold of $q = 15\ MeV/c$, so that we used the ratio of the fourth excited state at E^* = 17.64 MeV and the first excited state at E^* = 3.04 MeV for the temperature determination. The disadvantage of this thermometer is a rather small yield of ^{8}Be resulting in large statistical uncertainties. Thus the apparent ^{8}Be–temperature was determined without any centrality selection criterium.

For the ^{6}Li thermometer we have chosen the ratio of the 4.31 MeV and 5.65 MeV to the 2.17 MeV state. All three states decay into d–α (Fig. 5 lower right panel). Both resonances of ^{6}Li were described with a Breit–Wigner function (see Fig. 4). Because of the small energy difference strong feeding distortions of the ^{6}Li population are expected. Additionally a small change in the the background correlation function results in a big change of the relative yields due to the large values of the background yields resulting in large systematic errors. No centrality selection criterium was applied on the ^{6}Li thermometer.

The ^{5}Li thermometer yields a rather constant apparent temperature of $T \approx 5$ MeV

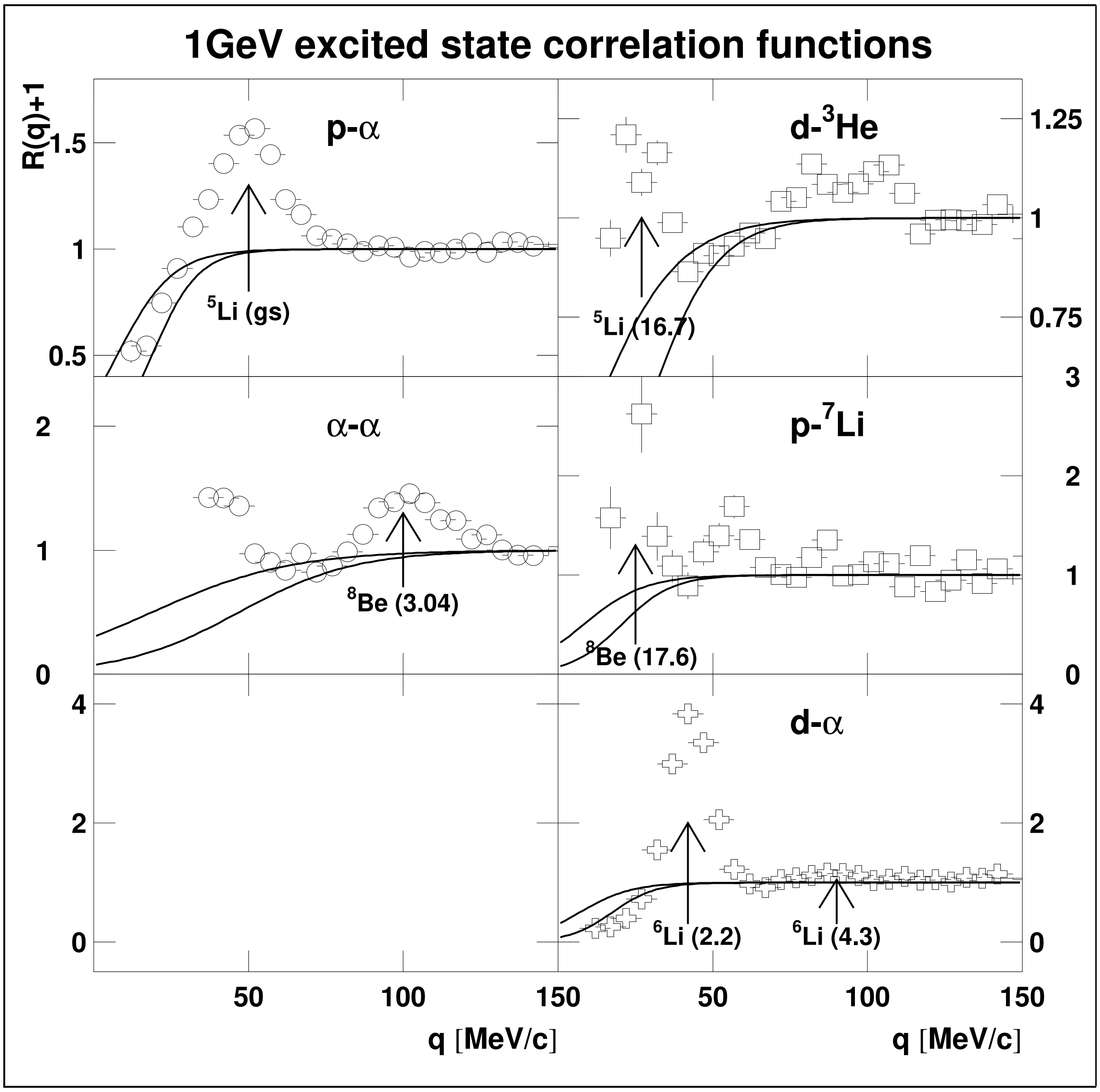

Figure 5: **First row:** *Ground state (p–α, left) and first excited state (d–^{3}He, right) of ^{5}Li* **Second row:** *Ground and first excited state (α–α, left), fourth to sixth excited state (p–^{7}Li, right) of ^{8}Be*
Third row: *First, third and fifth excited state of (d–α, right) of ^{6}Li*

independent of impact parameter (Fig. 6). The apparent temperature values are in the same range as reported elsewhere [10, 11, 12, 13, 14].

On the other hand, the extracted apparent temperature does not show a systematic rise as does the temperature T_{HeLi}, which was derived from the relative isotope ratios of Helium and Lithium [6] (open circles in Fig. 6).

For ^{5}Li the dependence on the kinetic energy of the particle pair was also investigated but no systematic trend could be established.

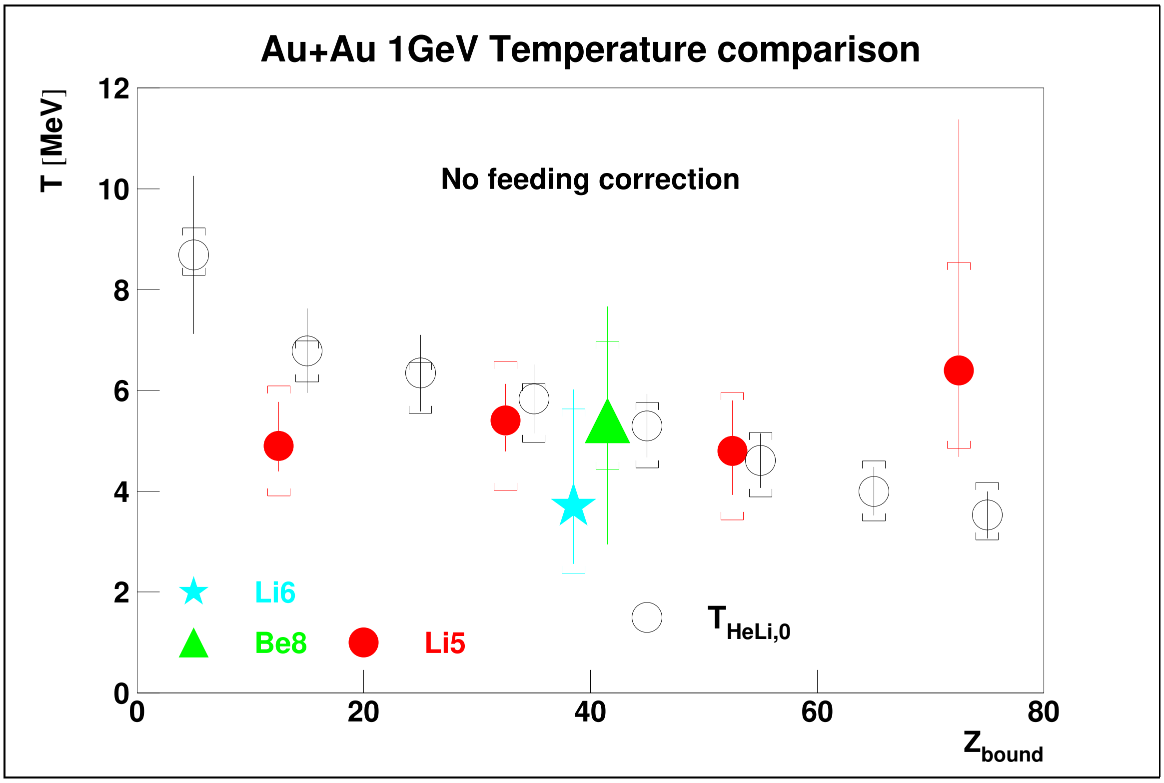

Figure 6: *Apparent temperatures from excited states for different thermometers vs* $Z_{\rm bound}$ *and comparison with isotope thermometer* $T_{\rm HeLi}$ *from the target spectator without feeding correction — The error bars represent the statistical uncertainty, the systematic uncertainty is indicated by the brackets*

4 Freeze out density from p–p and d–α correlations

In the first row of Fig. 7 the p–p correlation function for four different cuts in $\mathrm{Z_{bound}}$ together with a simulation from the Koonin–Pratt–formalism [15] for $r_0 = 8.0, 8.5, 9.0, 9.5$ fm and $\tau = 0$ fm/c is shown.

The peak height of d–α and p–α correlations should also be sensitive on the freeze out radius [16, 17]. The dependence of those on $\mathrm{Z_{bound}}$ is shown in the second and third row of Fig. 7. For the d–α correlations the integral of the first and second maximum was compared to the integral of theoretical d–α correlation functions [11, 16, 17] in order to get absolute numbers for the d–α freeze out radius. The hard sphere radii vary from 10 fm for $\mathrm{Z_{bound}} < 20$ to 11 fm for $\mathrm{Z_{bound}} > 60$.

Taking into account the increasing mass of the target spectator A_0 with increasing impact parameter we determined a mean freeze out density. This mean freeze out density varies from $0.2\rho_0$ ($0.17\rho_0$) in peripheral to $0.1\rho_0$ ($0.07\rho_0$) in central collisions for the p–p (d–α) correlations (fourth row of Fig. 7). These densities are smaller than the standard density of $0.3\rho_0$ which is usually used in theoretical calculations. A freeze out density which decreases with decreasing impact parameter was already proposed by [18] from INC calculations.

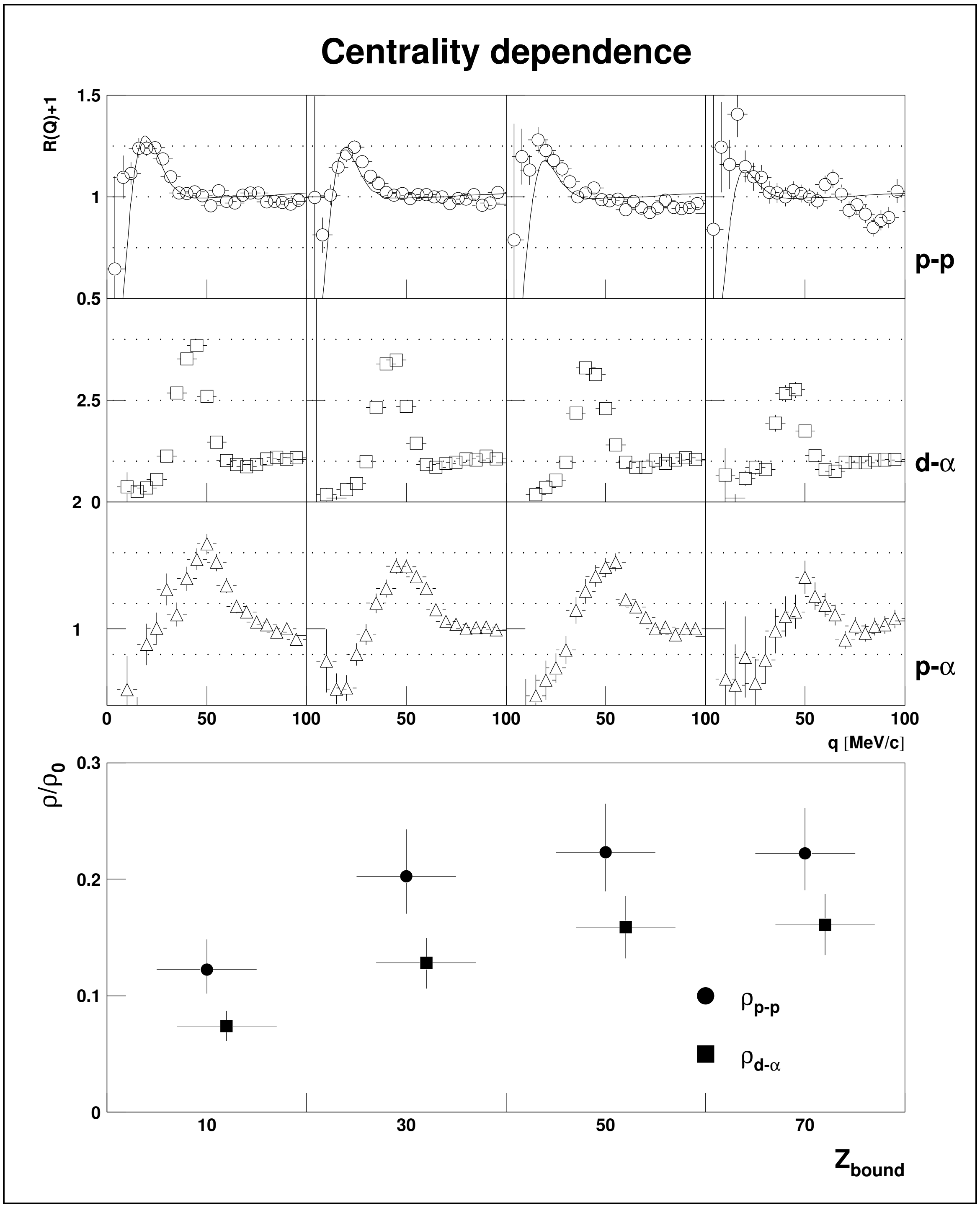

Figure 7: **First row:** *p–p correlation function for four different cuts in* Z_{bound} *(see x axis on fourth row) and comparison to simulated correlation functions for* $r_0 = 8.0 - 9.5$ *fm respectively*
Second row: *d–α correlation function for the same cuts as p–p in* Z_{bound}
Third row: *p–α correlation function for the same cuts as p–p in* Z_{bound}
Fourth row: *Mean density from extracted radii and prefragment mass* A_0 *vs* Z_{bound}

In Fig. 8 p–p, d–α and p–α correlations are shown for for three different ranges of summed energy. The peak heights of the correlation functions and as a consequence the extracted radii vary strongly with the summed energy of the particle pairs (Fig. 8). Faster particles seem to be emitted from a smaller source. This may be interpreted as a time ordered emission during expansion.

5 Comparison to Feeding calculations

For the analysis of feeding distortions we used the QSM code [19]. The **Q**uantum **S**tatistical **M**odel is based on the assumption of thermal and chemical equilibrium. This model incorporates infinite system size. The ground and excited states of nuclear states up to $Z = 13$ are included according to published values [9]. No continuous states are included in the QSM. The excluded volume of a fragment is the sum of the nucleon volumes (^{3}H and ^{3}He have the same excluded volume). The states are populated according to one global temperature T, density ρ and N/Z ratio. The initial particle ratios are modified due to the sequential decay of particle unbound states (feeding) and one has to distinguish between an initial and a final distribution. The final ratio was used to calculate yields of ground and excited particle unbound states. By applying the exponential temperature formula (equation 1) we derived a relationship between the initial temperature and the apparent ^{5}Li, ^{8}Be and ^{6}Li temperature respectively. The comparison of the experimental yield with the QSM calculation gives the following results:

1. The constant correction factor for the T_{HeLi} thermometer of 1.2 used by [1] was determined assuming a constant freeze out density $\rho = \rho_0/3$. However, the extracted freeze out radii from d–α correlations measured in the same experiment can best be described with a density varying from $0.17\rho_0$ for the most peripheral to $0.07\rho_0$ for the most central collisions. Because of the density dependence of the QSM correction the correction factor for the isotope thermometer becomes centrality dependent ranging from 1.2 for the most peripheral to almost 1 for the most central collisions. This reduces the observed effect of a steep rise in temperature for the most central collisions. The T_{HeLi} thermometer before and after QSM correction is shown in Fig. 9.

2. According to QSM there is no feeding correction factor needed for the extraction of the ^{5}Li temperature. Thus within QSM and the assumption of a global freeze out for all particle species only part of the discrepancy between excited state and isotope temperatures can be explained.

3. Additional feeding calculations for the ^{5}Li thermometer were performed analogous to [20] (see also [21]). The correction for the ^{5}Li thermometer from this code is less than 1 MeV.

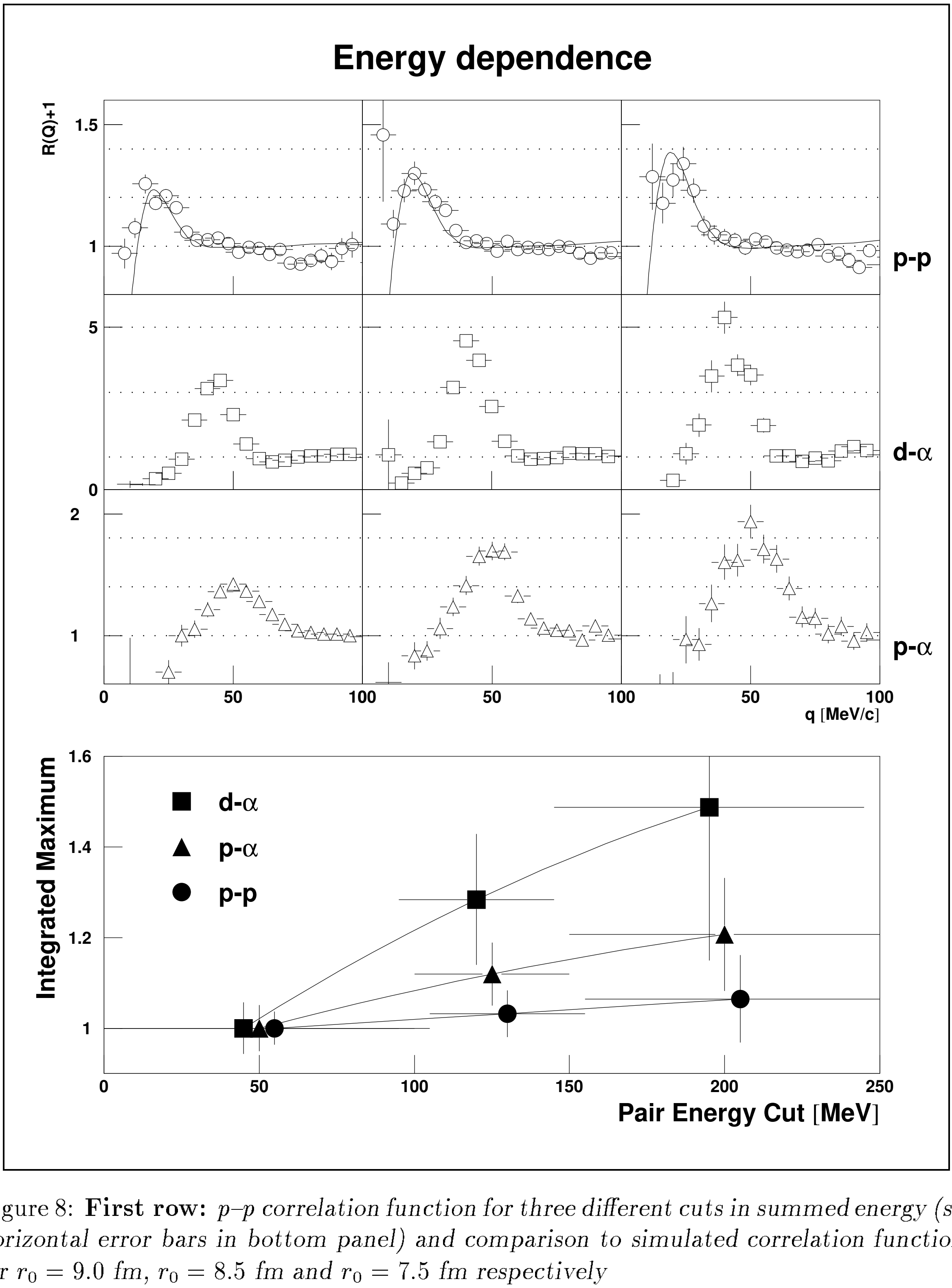

Figure 8: **First row:** *p–p correlation function for three different cuts in summed energy (see horizontal error bars in bottom panel) and comparison to simulated correlation functions for $r_0 = 9.0$ fm, $r_0 = 8.5$ fm and $r_0 = 7.5$ fm respectively*
Second row: *d–α correlation function for the same cuts as p–p in summed energy*
Third row: *p–α correlation function for the same cuts as p–p in summed energy*
Fourth row: *Rise of the integrated maximum in the correlation function with the summed energy for p–p, d–α and p–α correlations*

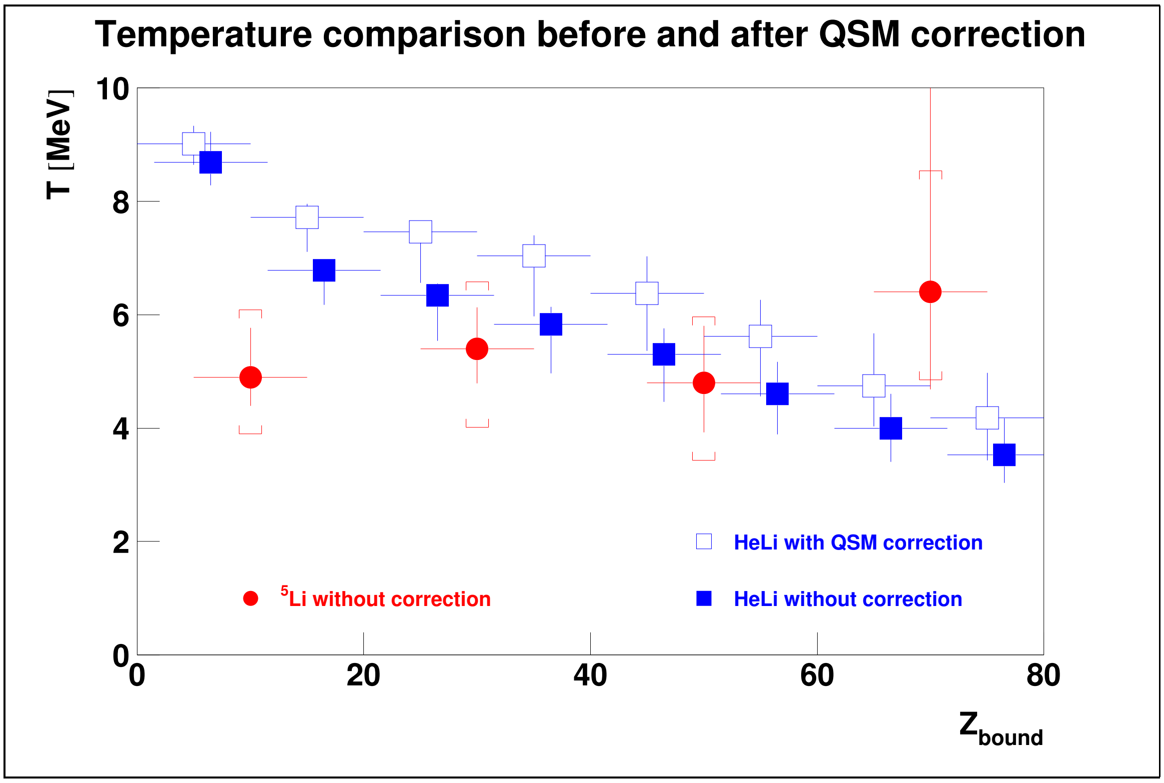

Figure 9: T_{HeLi} *before and after density dependent feeding correction according to QSM and comparison to apparent* ^{5}*Li temperature*

Summary

The extraction of apparent temperatures from of excited state population ratios for the system Au+Au at 1 A·GeV was presented and temperature values of $T \approx 5$ MeV are derived. In contrast to the isotope thermometer presented in [1, 6] the apparent temperature stays constant with decreasing impact parameter thus increasing excitation energy. The freeze out densities extracted by the means of d–α correlations and used as input for QSM calculations seem to favour a decreasing freeze out density with increasing excitation energy. After feeding correction one gets a rather slow rise in emission temperature starting at $T = 5$ MeV for the most peripheral and reaching around $T = 9$ MeV for the most central collisions with the isotope thermometer while the excited state thermometer saturates around $T \approx 6$ MeV emission temperature. This discrepancy is even more pronounced in Ref. [22] and explained by different freeze out times for isotope and excited state thermometers.

References

[1] J. Pochodzalla et al., Phys. Rev. Lett. 75 (1995) 1040.

[2] C.J.W. Twenhöfel, NIM B51 (1990) 58.

[3] A. Schüttauf et al., Nucl. Phys. A607 (1996) 457.

[4] C. Groß, PhD thesis, J.W.Goethe–Universität Frankfurt, 1997 (unpublished).

[5] W. Bauer, Phys. Rev. C51 (1995) 803.

[6] W. Trautmann, contribution to this Proceedings

[7] G.I. Kopylov, Phys. Lett. B50 (1974) 472.

[8] V. Serfling, PhD thesis, J.W.Goethe–Universität Frankfurt, 1997 (unpublished).

[9] F. Ajzenberg-Selove,
Nucl. Phys. A413 (1984) 28.
Nucl. Phys. A490 (1988) 1.

[10] J. Pochodzalla et al.,
Phys. Rev. Lett. 55 (1985) 177.
Phys. Lett. 161 B (1985) 275.

[11] J. Pochodzalla et al., Phys. Rev. C35 (1987) 1695.

[12] G.J. Kunde et al., Phys. Lett. B272 (1991) 202.

[13] T.K. Nayak et al., Phys. Rev. C45 (1992) 132.

[14] C. Schwarz et al., Phys. Rev. C48 (1993) 676.

[15] S.E. Koonin, Phys. Lett. 70B (1977) 43.
S. Pratt and M.B. Tsang, Phys. Rev. C36 (1987) 390.

[16] D.H. Boal and J.C. Shillcock, Phys. Rev. C33 (1986) 549.

[17] D.H. Boal, C.K. Gelbke an B.K. Jennings, Rev. of Mod. Phys.62 (1990) 553.

[18] P. G. Warren et al., Nucl-Ex–9610008 (1996).

[19] D. Hahn and H. Stöcker, Nucl. Phys. A476 (1988) 718.

[20] X. Hongfei, W.G. Lynch, M.B. Tsang, W.A. Friedmann, MSUCL-1040 (1996).

[21] B. Tsang, contribution to this Proceedings

[22] C. Schwarz, contribution to this Proceedings